Proceedings of the ASME 2014 International Mechanical Engineering Congress & Exposition
IMECE 2014
November 14-20, 2014, Montreal, Canada

IMECE2014-37302

DYNAMICS OF THIN LIQUID BILAYERS SUBJECTED TO AN EXTERNAL ELECTRIC FIELD

Hadi Nazaripoor*
Dept. of Mechanical Engineering
University of Alberta
Edmonton, AB, Canada T6G 2G8
Email: hadi@ualberta.ca

Charles R. Koch
Dept. of Mechanical Engineering
University of Alberta
Edmonton, AB, Canada T6G 2G8

Subir Bhattacharjee
Water Planet Engineering
721 Glasgow Ave, Unit D
Inglewood, California, 90301, USA

ABSTRACT

Spatiotemporal evolution of liquid-liquid interface leading to dewetting and pattern formation is investigated for thin liquid bilayeres subjected to the long range electrostatic force and the short range van der Waals forces. Based on the 2D weakly nonlinear thin film equation three dimensional structure evolution is numerically simulated. A combined finite difference for the spatial dimensions and an adaptive time step ODE solver is used to solve the governing equation. For initially non-wetting surfaces, the stabilizing effects of viscosity and interfacial tension and the destabilizing effect of the Hamaker constant are investigated. Electrostatic interaction is calculated analytically for both perfect dielectric-perfect dielectric and ionic conductive-perfect dielectric bilayers. Ionic conductive-perfect dielectric bilayers based on the electric permittivity ratio of layers are found to be stabilized or deformed in response to the applied external electric field.

INTRODUCTION

Dynamics of ultra-thin ($< 500nm$) liquid films on solid substrates has gained significant attention due to its interesting behavior and its numerous technological applications [1–6]. Instabilities in thin liquid films caused by van der Waals forces or external stimuli like thermal, mechanical and electrical forces lead to dewetting and pattern formation of films [7–12]. Development of these instabilities at the liquid film interface gives rise to the film disruption and/or pattern formation on the film interface, which is of interest in numerous applications.

Determining drainage time (i.e. time when film's rupture occurs) and different morphological structures of the film interface requires insight into the dynamics and morphological evolution of the film. From bulk fluid dynamics, interfacial tension and viscosity are known as damping factors for fluctuations on the free surfaces. Small scale systems also have intermolecular forces which depend on material properties of the films and substrate, and these forces play a dominant role in engendering instability of thin films [13, 14]. These intermolecular interactions create a pressure, called the conjoining pressure, on the film interface [3]. The stability of the thin film depends on the first derivative of the conjoining pressure with respect to the local film thickness, often referred to as the spinodal parameter. When there are no strong residual stresses in the films [5], in apolar systems (systems under consideration in this study) the conjoining pressure has only one component (van der Waals interaction) and the sign is determined by the sign of system's effective Hamaker constant.

More recently, electrically induced perturbations of thin films leading to micro/nano structures formation, known as electrohydrodynamic (EHD) patterning, has also received considerable attention [15–20]. In this process, an electric field is applied to the thin film sandwiched between two electrodes (see Fig.1). The electrostatic force acts on the film interface because of the discontinuous electric fields acting on the two sides of the liquid interface [21]. This results in complex interface dynamics and the potential to create complex shapes in the fluid

*Corresponding author.

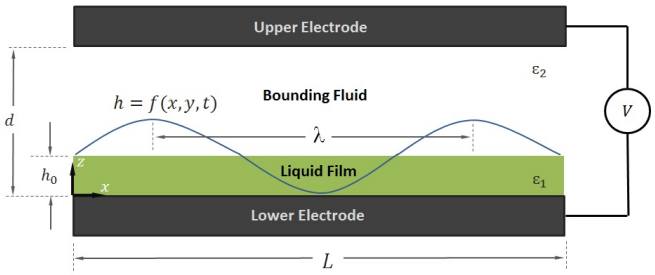

FIGURE 1. Schematic representation of a bilayer (thin liquid film-bounding fluid) sandwiched between two electrodes. λ is wavelength of growing instabilities on the interface.

layer. The shape and size of structures are determined by geometrical (filling ratio and electrodes shape, etc.) and electrostatic (relative electric permittivity of layers and applied voltage, etc.) properties of the system [16, 19]. Pillars, bicontinuous, holes and undulating structures are observed on the bilayer-two adjoining immiscible liquid layers with a common deformable interface having electrical, apolar, and fluid mechanical property discontinuities-interface based on the electric permittivity ratio of layers and their initial filling ratio-film thickness to the electrodes distance ratio [16, 22]. Initially, growth of instabilities are found to be linear and linear stability analysis (LS) is used to characterize the interface behavior. This changed to nonlinear for later times [23].

It has been experimentally observed that a hexagonal pillar pattern forms on the interface with a centre-to-centre distance equal to fastest growing wavelength of instabilities, λ_{max}, predicted by LS [15]. To produce smaller features (reducing λ_{max}) in EHD patterning technique like applied voltage V, film initial thickness h_0, electrodes distance d, conductivity σ and electric permittivity of layers ε have been examined [16, 22, 24]. Replacing the upper layer (i.e bounding fluid) with an ionic conductive media leads to higher electrostatic force acting on the interface as less electric potential drop occurs within upper layer and so the film is subject to a higher electric field. Experiments show that using an ionic liquid upper layer leads to smaller size pillars that are disordered and polydispersed (the pattern is not hexagonal) [18]. Film drainage, dewetting of surfaces and pattern formation on the interface has been extensively studied using linear stability analysis or 3D nonlinear simulations. However, film drainage and its dynamics where there is an interaction between short range van der Waals and long range electrostatic forces, and nonlinear structure selection or its morphological evolution control in confined bilayers have not been comprehensively studied.

In this study, the non-linear spatio-temporal evolution of a liquid-liquid interface under the combined influence of electrostatic and apolar interactions is investigated. The electrostatic interaction is calculated analytically for both perfect dielectric-perfect dielectric (PD-PD) and ionic conductive-perfect dielectric (IC-PD) bilayers.

TABLE 1. Constants or parameters used in simulations.

Parameter	Value
interfacial tension (γ)	$0.002-0.06$ $\frac{N}{m}$
viscosity of liquid film (μ)	$1-100$ Pa s
effective Hamaker constant (A)	$(-)$ $10^{-21}-10^{-18}$ J
permittivity of vacuum (ε_0)	8.85×10^{-12} $\frac{C}{V\,m}$
electric permittivity of the liquid film (ε_1)	2.5 $(-)$
electric permittivity ratio of layers (ε_r)	$0.1-1.5$ $(-)$
initial film thickness (h_0)	$5-20$ nm
electrodes distance (d)	100 nm
equilibrium distance (l_0)	$1-5$ nm
applied voltage (V_{up})	$0-20$ V

MATHEMATICAL MODEL

A schematic of thin liquid-liquid bilayer (liquid film-bounding fluid) resting on a solid substrate and confined to a flat upper electrode is shown in Fig.1. The material properties of liquid layers such as dielectric constant and viscosity are assumed constant. Constants and parameters used in this study are listed in Table 1. Liquid layers are assumed Newtonian, incompressible, isothermal, immiscible and thin enough to neglect the gravity effects. Thin film evolution is described using continuity and Navier-Stokes (NS) equations for both liquid film and bounding fluid.

$$\nabla.\vec{u}_i = 0 \tag{1}$$

$$\rho_i(\frac{\partial \vec{u}_i}{\partial t} + (\vec{u}_i.\nabla\vec{u}_i)) = -\nabla P_i + \nabla.[\mu_i(\nabla\vec{u}_i + (\nabla\vec{u}_i)^T)] + \vec{f}_e \tag{2}$$

Where $\vec{f}_e = -\nabla\phi$ is for external body force, ϕ is conjoining pressure, $i = 1,2$ stands for i^{th} fluid phase. Boundary conditions are:

$$\vec{u}_i = 0 \qquad at\ \ z = 0\ \ \&\ \ z = d \tag{3}$$

$$\vec{u}_{relative} = 0 \qquad at\ \ z = h(x,y,t) \tag{4}$$

Kinematic boundary condition is used to relate interfacial velocity component to the film thickness as [23]

$$w = \frac{\partial h}{\partial t} + u\frac{\partial h}{\partial x} + v\frac{\partial h}{\partial y} \quad at \quad z = h(x,y,t) \tag{5}$$

To simplify and solve the governing equations, it is assumed (a) the upper layer is much less viscous than the lower layer, (b) liquid film is thin enough to neglect the inertial effects. Since the mean film thickness is significantly smaller than the characteristic wavelengths of the disturbance (i.e. $h_0/\lambda \ll 1$) [9], the long-wave approximation is used to find spatio-temporal evolution of the thin film height.

$$3\mu h_t + [h^3(\gamma[h_{xx}+h_{yy}]-\phi)_x]_x + [h^3(\gamma[h_{xx}+h_{yy}]-\phi)_y]_y = 0 \tag{6}$$

where x and y subscripts denote for derivatives with respect to x and y. Greater details and governing equations are available in other references [3, 16, 19, 25]. The conjoining pressure ϕ is the summation of all excess intermolecular interactions that exist in the system. In general, it is defined as $\phi = \phi_{vdW} + \phi_{Br} + \phi_E$. The term, ϕ_{vdW}, is van der Waals component of excess pressure and given by $\phi_{vdW} = A/6\pi h^3$ [13, 14] and A is the effective Hamaker constant for the layered three components system in Fig.1 $A_{213} = (\sqrt{A_{33}} - \sqrt{A_{11}})(\sqrt{A_{22}} - \sqrt{A_{11}})$ in which 1,2 and 3 denote substrate, liquid film and bounding fluid, respectively. The second term is for the Born repulsive force for the lower and upper electrode, $\phi_{Br_L} = -8B_L/h^9$ and $\phi_{Br_U} = 8B_U/(d-h)^9$ and is used to remove the contact line singularity in case of dewetting and wetting of lower and upper electrodes [16, 19]. Coefficients B_L and B_U are calculated by equating the net conjoining pressure equal to zero at equilibrium distance l_0 from the lower and upper electrodes. The electrostatic conjoining pressure, ϕ_E is developed due to the Maxwell stress induced at the fluid interface [21] requires the calculation of electric potential. Governing equation for electric potential in the perfect dielectric layer with no free charge is the Laplace equation and in the ionic conductive layer is the Poission equation. Governing equations for electric potential (V_i , i=1 and 2 for thin film and bounding fluid, respectively.) in the long-wave limit are

$$\partial^2 V_1/\partial z^2 = 0 \;\; ; \;\; \partial^2 V_2/\partial z^2 = \frac{-\rho_{f_2}}{\varepsilon_2 \varepsilon_0} \tag{7}$$

and the boundary conditions are

$$V_1 = 0 \;\; at \; z = 0 \quad ; \quad V_2 = V \quad at \; z = d$$
$$V_1 = V_2 \;\; and \;\; \varepsilon_1(\partial V_1/\partial z) = \varepsilon_2(\partial V_2/\partial z) \;\; at \; z = h(x,y,t) \tag{8}$$

Charge density in ionic conductive layer, ρ_{f_2}, in pseudo-steady [18] and equilibrium condition for symmetric monovalent condition [13] is given by

$$\rho_{f_2} = 2000 e N_A M \sinh[-\frac{e(V - V_{up})}{k_B T}] \tag{9}$$

where, e is the magnitude of electron charge and M is electrolyte molar concentration (mol/L). N_A is Avogadro number, k_B is the Boltzmann constant and T is the temperature in (K). Using this definition for charge density leads to Poisson-Boltzmann equation for ionic conductive liquid layer. Electric potential distribution is found by solving the Eqns. 7,8 and 9 and finally the electrostatic conjoining pressure is obtained as

$$\phi_E = -\frac{1}{2}\varepsilon_0 \varepsilon_1 (\varepsilon_r - 1) {E_1}^2 \tag{10}$$

Electric field in the film, E_1, for the case of PD-PD bilayers ($\rho_{f_2} = 0$)

$$E_1 = \frac{V_{up}}{h(1-\varepsilon_r) + \varepsilon_r d} \tag{11}$$

and for IL-PD bilayers

$$E_1 = \frac{V_s}{h} \tag{12}$$

where, V_s is the electric potential at the bilayer interface is obtained by solving the following nonlinear equation for each interface height $h(x,y,t)$

$$\varepsilon_r V_s - h(\frac{\varepsilon_2 k_B T}{500 e^2 N_A M})^{1/2} \sinh(\frac{V_s - V_{up}}{2}) = 0 \tag{13}$$

Scaling

For LS analysis following problem scaling is used:

$$\lambda_{max} = 2\pi\sqrt{\frac{2\gamma}{|\frac{\partial\phi}{\partial h}|}}$$

$$x^*, y^* = \lambda_{max} \quad \& \quad t^* = \frac{12\mu\gamma}{h_0^3(\frac{\partial\phi}{\partial h})^2} \quad at \quad h = h_0 \tag{14}$$

In Eq.14, ϕ is the initial dominant excess pressure in the system (i.e. ϕ_{vdW} for pressure based and ϕ_E for electric based drainage) [3, 15, 16, 24]. Interface height is also scaled with lower layer mean initial thickness, $H(x^*, y^*, t^*) = h(x, y, t)/h_0$.

Numerical method

Based on the 2D weakly nonlinear thin film equation (Eq. 6) the 3D liquid film height evolution is numerically simulated over a square domain with periodic boundary conditions. A finite difference in space combined with and an adaptive time step ODE solver is used. Simulations were started with small random but volume preservative disturbances at the interface. Uniform Cartesian grids with 61×61 and 121×121 spatial grids for the domain sizes of 4 λ_{max}^2 and $16\lambda_{max}^2$ are found sufficient to track bilayer interface and used throughout this study. The smaller domain size is used to study the drainage time whereas for the patterns evolution the larger domain is used. A custom Fortran code is used.

RESULTS AND DISCUSSION

First for the base case, the behavior of thin liquid bilayer drainage under no external electric field is addressed. To do this an initially unstable thin liquid bilayer system with properties listed in Table 1 is selected. Then the stabilizing effects of lower layer viscosity and interfacial tension and the destabilizing effect of the Hamaker constant are investigated. Film drainage and the spatiotemporal evolution of the interface are presented to track the morphology and dewetting of liquid-liquid bilayer in response to short range van der Waals forces. These simulations are done for an initially unstable film under no external electric disturbance. Next, for an applied electric field, the effects of variations in the electric permittivity ratio of bilayers (ε_r) on the pattern formation, as well as the feature shape and size are studied. Finally the effect of using a bounding fluid which is IC instead of being PD is tested to understand it's effects on the dynamics and pattern formation process. These results will be discussed in this section.

Nondimensional minimum film thickness variations versus time by changing (a) interfacial tension and (b) film viscosity is shown in Fig.2. The lowest value for the interface height is the

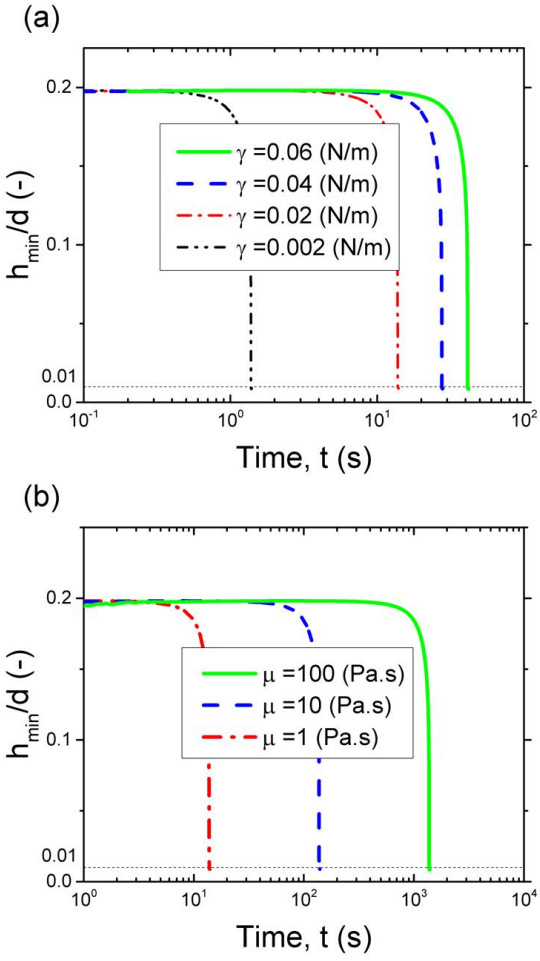

FIGURE 2. Nondimensional minimum film thickness variations on an initially unstable bilayer under no applied electric field versus time for: (a) interfacial tension, γ and (b) viscosity, μ. $A = 10^{-19}(J)$

equilibrium distance defined for the Born repulsive force on the lower electrode. This is used to avoid a contact line singularity and is shown with dotted line in $h_{min}/d = 0.01$. The time when the interface reaches the Born equilibrium height is defined as the drainage time and it gives an indication as to how fast instabilities are growing over the domain. In Fig.2a surface tension is varied at $\mu = 1(Pa.s)$ while in Fig.2b viscosity is varied at $\gamma = 0.02(N/m)$. Drainage time increases by several orders of magnitude for both increasing surface tension and viscosity. Presenting the results in dimensional time assists in better understanding of these considerable effects in the real time experiments. The use of low viscosity polymers degrade damping of fluctuations and leads to fast dewetting and pattern formations in films which is of interest in fast EHD patterning.

Attractive van der Waals forces (effective Hamaker constant

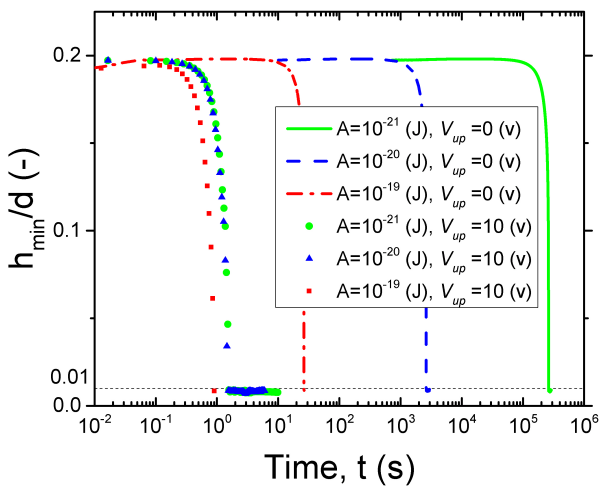

FIGURE 3. Nondimensional minimum film thickness variations on an initially unstable bilayer versus time: Effects of hamaker constant, A, and applied voltage, V_{up}.

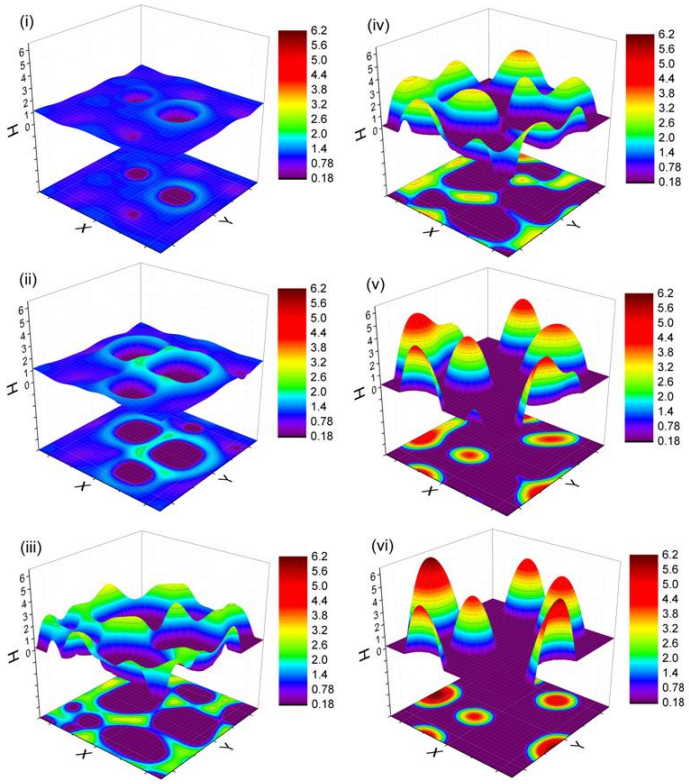

FIGURE 4. Major stages for time evolution of patterns, nondimensional times are t^*=29, 30, 32, 33, 35 and 40. $h_0 = 5$ nm and $A = 1.5 \times 10^{-19}(J)$.

greater than zero) tend to enhance fluctuation growth. Systems with higher effective Hamaker constant are more unstable and film rupture occurs sooner in these systems as shown in Fig.3. The film drainage time is more sensitive to Hamaker constant when no electrostatic force ($V_{up} = 0$) is applied. This is illustrated by the $V_{up} = 0$ lines in Fig.3. By applying electric field, electrostatic stress forms on the interface due to inequality of electric permittivity ratio of layers ($\varepsilon_r = 2.5$) and this force is considered as a long range and dominant force compared with van der Waals forces. Drainage time significantly decreases when applying a voltage but still depends on the Hamaker constant value. However the drainage time is not sensitive to the Hamaker constant in presence of electrostatic force.

Nondimensional film thickness as a function of time shows how the initial disturbances grow during the early stages of pattern formation. A sequence of times (t^*) are used to show the different stages in the dewetting process of an initially unstable film as illustrated in Fig.4 with no applied electric field. The initial random disturbance is reorganized into nonuniform holes (see Fig.4 (i)) then holes and their surrounded uneven rims are expand over time (see Fig.4 (ii)) leading to holes coalescence and bicontinuous structure formation (see Fig.4 (iii)). Next, long undulating (peak and valley) shape structures form due to coalescence of holes and undergo some fragmentation and create droplets (see Fig.4 (iv-v)). The size of droplets increases over time (see Fig.4 (vi)) due to negative diffusion-fluid flow from thinner region to the thicker region. Finally droplets coalesce to minimize the interface area and form one droplet in the final equilibrium condition (image is not shown).

The effects of the electric permittivity ratio variations on the stability, dynamics and pattern formation on the bilayer interface are shown in Fig.5 and 6, respectively, two ratios of $\varepsilon_r = 1.5$ and 0.1. For $\varepsilon_r = 1.5$, the electrostatic force (see Eq.10) is pushing the interface toward the upper electrode (denoted disjoining) and for $\varepsilon_r = 0.1$, electrostatic force is pushing the interface toward the lower electrode (denoted conjoining). For a thin film that is initially stable (Hamaker constant is less than zero) the electrostatic force can either enhance or lower the stability of a liquid-liquid interface.

Figure 5 shows two stages of the pattern formation on the interface in a(i and ii) PD-PD and b(i and ii) IC-PD bilayers. In bilayers with an electric permittivity ratio greater than one when the upper layer is perfect dielectric, pillar structures with circular cross sections are created. In an ionic conductive (IC) upper layer case initial random disturbances are damped over time. This shows that the electrostatic force is stabilizing the perturbations in this case. As mentioned earlier, negative diffusion is a driving mechanism in systems where spinodal parameter is nega-

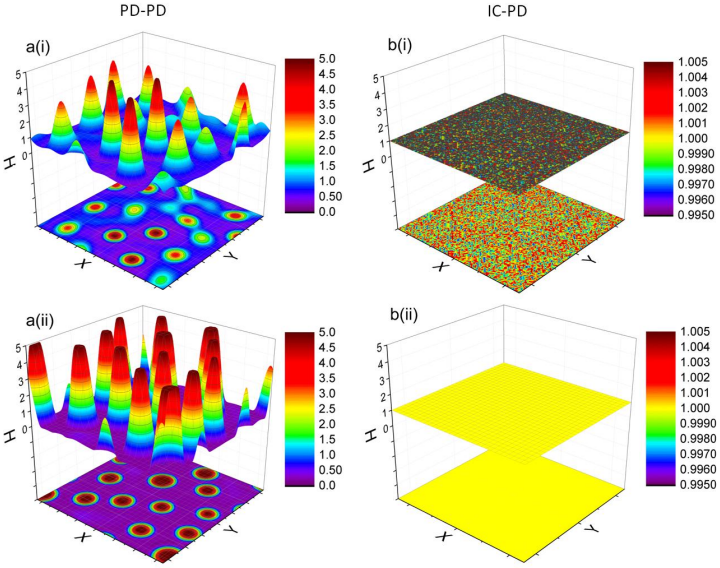

FIGURE 5. Stages for time evolution of patterns a(i and ii) PD-PD and b(i and ii) IC-PD bilayer, nondimensional times are t^*= a(i) 3.88×10^6, a(ii) 8.37×10^6, b(i) 0 and b(ii) 91, $h_0 = 20$ nm and $A = -1.5\times10^{-20}(J)$.

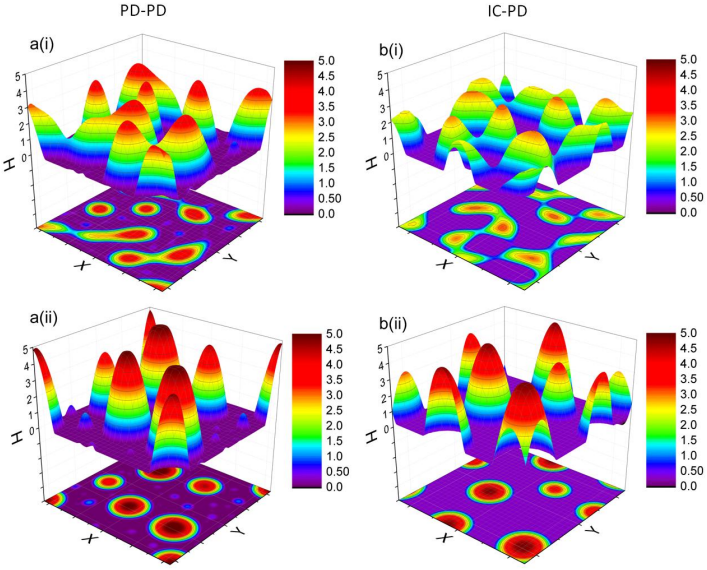

FIGURE 6. Stages for time evolution of patterns a(i and ii) PD-PD and b(i and ii) IC-PD bilayer, nondimensional times are t^*= a(i)125, a(ii) 200, b(i) 11 and b(ii) 15.4, $h_0 = 20$ nm and $A = -1.5\times10^{-20}(J)$.

tive. The spinodal parameter for PD-PD bilayers are unstable for both $\varepsilon_r > 1$ and $\varepsilon_r < 1$ ranges, while IC-PD bilayers are only unstable while $\varepsilon_r < 1$. For IC-PD bilayers with $\varepsilon_r > 1$, the spinodal parameter is positive predicting a stabilizing effect for electrostatic force.

Two stages of pattern formation on the interface of PD-PD and IC-PD bilayers with the $\varepsilon_r = 0.1$ are shown in Fig.6. Pillars are formed on the interface of both PD-PD and IC-PD condition (see Fig.6 a(ii) and b(ii)) and fragmentation of long hills shape structures is seen before the pillars formation (see Fig.6 a(i) and b(i)) similar to those seen in dewetting of films under attractive van der Waals forces (see Fig.4 (iv) and (v)). Here, pillars are polydispersed compared to those formed in PD-PD with$\varepsilon_r = 1.5$ in which they have the typical hexagonal structure [15]. However, from the LS calculations for λ_{max} the size of pillars for $\varepsilon_r = 0.1$ are much smaller than those obtained in $\varepsilon_r = 1.5$. So the number of pillars that form in $\varepsilon_r < 1$ are much higher than for bilayers with $\varepsilon_r > 1$ with the same physical domain.

CONCLUSION

This paper has addressed dynamics and spatiotemporal evolution of liquid-liquid interface leading to dewetting and pattern formation for thin liquid bilayeres subjected to the long range electrostatic force and the short range van der Waals forces. Based on the 2D weakly nonlinear thin film equation, three dimensional structure evolution is numerically simulated. A combined finite difference for the spatial dimensions and an adaptive time step ODE solver is used. The stabilizing effects of viscosity and interfacial tension and the destabilizing effect of the Hamaker constant are investigated by assessing thin film's drainage and the spatiotemporal evolution of interface. The morphology and dewetting of liquid-liquid bilayer in presence of attractive short range van der Waals forces is investigated. Then the dynamics, stability and morphology of electrically induced perturbation of the interface are examined for both PD-PD and IC-PD bilayers based on the analytical results obtained for electrostatic conjoining pressures. Bilayers with $\varepsilon_r < 1$ have smaller size pillars compared with $\varepsilon_r > 1$ case. Using upper IC media instead of PD as a bounding fluid decreases the size of pillars though they are polydispersed. It is also observed that electrostatic force stabilizes the initial perturbations in IC-PD bilayers with $\varepsilon_r > 1$.

ACKNOWLEDGMENT

We acknowledge financial support from the Natural Sciences and Engineering Research Council (NSERC), Canada, Chair in Water Quality Management for Oil Sands Extraction, the Alberta Water Research Institute (AWRI), Kemira, Outotec, Suncor Energy, Statoil and ConocoPhilips. H.N. acknowledges financial support from the University of Alberta Doctoral Recruitment Scholarship.

REFERENCES

[1] Ruckenstein, E., and Jain, R. K., 1974. "Spontaneous rupture of thin liquid films". *J. Chem. Soc., Faraday Trans. 2,* ***70***, pp. 132–147.

[2] Mitlin, V. S., 1993. "Dewetting of solid surface: Analogy with spinodal decomposition". *Journal of Colloid and Interface Science,* ***156***(2), pp. 491 – 497.

[3] Sharma, A., and Khanna, R., 1998. "Pattern formation in unstable thin liquid films". *Physical Review Letters,* ***81(16)***(10), pp. 3463–3466.

[4] Khanna, R., Agnihotri, N. K., Vashishtha, M., Sharma, A., Jaiswal, P. K., and Puri, S., 2010. "Kinetics of spinodal phase separation in unstable thin liquid films". *Phys. Rev. E,* ***82***, Jul, p. 011601.

[5] Thomas, K. R., Chenneviere, A., Reiter, G., and Steiner, U., 2011. "Nonequilibrium behavior of thin polymer films". *Phys. Rev. E,* ***83***, Feb, p. 021804.

[6] Roy, S., Biswas, D., Salunke, N., Das, A., Vutukuri, P., Singh, R., and Mukherjee, R., 2013. "Control of morphology in pattern directed dewetting of a thin polymer bilayer". *Macromolecules,* ***46***(3), pp. 935–948.

[7] Lin, S., and Brenner, H., 1982. "Marangoni convection in a tear film". *Journal of Colloid and Interface Science,* ***85***(1), pp. 59 – 65.

[8] A. Koulago, V. Shkadov, A. D. R., and Quere, D., 1995. "Film entertainment by a fibre quickly drawn out of a liquid bath". *Phys. Fluids,* ***7***, p. 1221.

[9] Oron, A., Davis, S. H., and Bankoff, S. G., 1997. "Long-scale evolution of thin liquid films". *Rev. Mod. Phys.,* ***69***, Jul, pp. 931–980.

[10] Quere, D., 1999. "Fluid coating on a fiber". *Annual Review of Fluid Mechanics,* ***31***, pp. 347–384.

[11] Eow, J. S., Ghadiri, M., Sharif, A. O., and Williams, T. J., 2001. "Electrostatic enhancement of coalescence of water droplets in oil: a review of the current understanding". *Chemical Engineering Journal,* ***84***(3), pp. 173 – 192.

[12] Mostowfi, F., Khristov, K., Czarnecki, J., Masliyah, J., and Bhattacharjee, S., 2007. "Electric field mediated breakdown of thin liquid films separating microscopic emulsion droplets". *Applied Physics Letters,* ***90***(18), pp. 184102–184102–3.

[13] Masliyah, J. H., and Bhattacharjee, S., 2006. *Electrokinetic and Colloid Transport Phenomena*. Wiley-Interscience.

[14] Israelachvili, J. N., 2011. *Intermolecular and Surface Forces*, third edition ed. Elsevier Inc.

[15] Schaffer, E., Thurn-Albrecht, T., Russell, T. P., and Steiner, U., 2000. "Electrically induced structure formation and pattern transfer". *Nature,* ***403***, pp. 874–877.

[16] Verma, R., Sharma, A., Kargupta, K., and Bhaumik, J., 2005. "Electric field induced instability and pattern formation in thin liquid films". *Langmuir,* ***21***(8), pp. 3710–3721.

[17] Wu, N., Kavousanakis, M. E., and Russel, W. B., 2010. "Coarsening in the electrohydrodynamic patterning of thin polymer films". *Phys. Rev. E,* ***81***, pp. 26306–19.

[18] Lau, C. Y., and Russel, W. B., 2011. "Fundamental limitations on ordered electrohydrodynamic patterning". *Macromolecules,* ***44***(19), pp. 7746–7751.

[19] Atta, A., Crawford, D. G., Koch, C. R., and Bhattacharjee, S., 2011. "Influence of electrostatic and chemical heterogeneity on the electric-field-induced destabilization of thin liquid films". *Langmuir,* ***27***(20), pp. 12472–12485.

[20] Liu, G., Yu, W., Li, H., Gao, J., Flynn, D., Kay, R. W., Cargill, S., Tonry, C., Patel, M. K., Bailey, C., and Desmulliez, M. P. Y., 2013. "Microstructure formation in a thick polymer by electrostatic-induced lithography". *Journal of Micromechanics and Microengineering,* ***23***(3), p. 035018.

[21] Landau, L. D., and Lifshitz, E. M., 1960. *Electrodynamics of continuous media*. Pergamon Press.

[22] Wu, N., and Russel, W. B., 2006. "Electrohydrodynamic instability of dielectric bilayers: kinetics and thermodynamics". *Industrial & Engineering Chemistry Research,* ***45***(16), pp. 5455–5465.

[23] Williams, M. B., and Davis, S. H., 1982. "Nonlinear theory of film rupture". *Journal of Colloid and Interface Science,* ***90***(1), pp. 220 – 228.

[24] Lin, Z., Kerle, T., Russell, T. P., Schffer, E., and Steiner, U., 2002. "Structure formation at the interface of liquid/liquid bilayer in electric field". *Macromolecules,* ***35***(10), pp. 3971–3976.

[25] Sharma, A., and Khanna, R., 1999. "Pattern formation in unstable thin liquid films under the influence of antagonistic short- and long-range forces". *Journal of Chemical Physics,* ***110***(10), pp. 4929–4936.